

Perception-aware Trajectory Planning for a Pair of Unicycle-like Robots with Absolute and Relative Ranging Measurements

Francesco Riz, Luigi Palopoli, Daniele Fontanelli

Abstract—We consider two “kidnapped” unicycle vehicles released in an unknown environment. Each one is in sight of a ranging sensor (anchor) and has to choose a trajectory that enables it to localise itself relying only on its anchor measurements, on its odometry and on the information (state and mutual distance) that it can exchange with the other vehicle when they are sufficiently close. We propose a motion planning algorithm that solves the simultaneous localisation problem in this challenging scenario.

Index Terms—Nonholonomic systems; Autonomous vehicles; Robotics

I. INTRODUCTION

Mobile robots are constantly increasing their capabilities to operate in different scenarios and to execute complex tasks. For many of their applications, robots are required to navigate across partially unknown and dynamic environments, for which it is essential to know their pose. Pose estimation algorithms can rely on different sensors to collect information and reduce the localisation uncertainty. One of the most robust and cheapest sensor used in mobile robotics is the so-called *ranging sensor*, i.e. a sensor measuring the distance between the robot and a fixed point in the space. Different techniques can be used to reconstruct this information from wireless emitters, such as Wi-Fi fingerprinting [1], Radio Frequency IDentification (RFID) [2], Ultra-Wide Band (UWB) [3]. These techniques are used in combination with a variety of passive tags or active sensors placed in the environment in known locations. In the rest of the paper, we will refer to these devices by the terms anchors, landmarks or markers. Because of the remarkable costs of deploying and maintaining the anchors, it is imperative to explore the minimal localisation abilities of a mobile robot when the deployed infrastructure is very lean. In our past work [4], [5], we have studied the problem from the perspective of a single agent that travels across an unknown environment and “occasionally” comes in sight of one anchor. In this paper, we take the first steps toward the extension of these results to a multi-robot system, in which the agents collect information from their anchors, and are themselves equipped with a “mobile” anchor that allows them to measure their mutual distance when they meet. We consider the challenging scenario in which two “kidnapped” agents, each one being within the range of an anchor but completely unaware of their position and orientation, need to develop a navigation

strategy to localise themselves when they meet. The main points made in this paper are twofold: 1. since each of the vehicles can rely only on a limited amount of information, i.e. measurements collected from its reference anchor, which are not sufficient to estimate the current position and orientation of the vehicle, the two vehicles need to meet and collect relative measurements in order to achieve *global constructibility*; 2. each vehicle can plan its next manoeuvres by simply relying on the (limited) information available at each time step.

Related work: Since ranging sensors are one of the most popular and widely used sensors in mobile robotics, due to their limited cost, observability analyses and active trajectory planning techniques have been developed in the technical literature. Cedervall et al. [6] present an active control technique, whereby the vehicle estimates its state. With the same *rationale*, Salaris et al. [7] propose a perception-aware control strategy maximising for local constructibility (see also [8]). These ideas are extended to multiagent systems in [9], where the vehicles use mutual range measurements to localise themselves in the environment. Range-based information have been used in [10], [11] to maximise observability (measured by the Fisher Information Matrix and by the Observability Matrix, respectively), while Mandić et al. [12] combine observability maximisation with the leader-follower idea. Active sensing techniques have also been used in multiagent system to improve the localisation estimate of the agents of the system itself, relying on bearing [13] or on ranging data [14].

The papers cited above deal with local properties based on the Gramians, the Fisher Information Matrix or on the Observability Matrix. Instead, we consider global observability properties and a peer-to-peer framework in which all the agents have the same role.

Paper contributions: We consider an environment equipped with 2 fixed-frame range sensors, where 2 unicycle vehicles are free to move. Each vehicle is completely unaware of its initial position and orientation and has to plan its trajectory to reconstruct its state only relying on the measurements from its “reference” anchor, on the manoeuvres executed, and on the mutual measurements and information exchanged with the other vehicle, available only when they come sufficiently close to each other. We propose a control strategy, based on three phases, allowing the two vehicles to avoid indistinguishability. In the first phase the robots execute some manoeuvres to extract the maximum information from the anchors. In the second phase, they follow circular trajectories, which (under appropriate assumptions) enable them to

F. Riz and L. Palopoli are with the Department of Information Engineering and Computer Science, University of Trento, Italy, e-mail: {francesco.riz, luigi.palopoli}@unitn.it.

D. Fontanelli is with the Department of Industrial Engineering, University of Trento, Italy, e-mail: daniele.fontanelli@unitn.it

meet. The third phase consists of a sequence of manoeuvres that enables the vehicles to rule out the remaining ambiguity.

II. BACKGROUND AND PROBLEM FORMULATION

We consider a pair of vehicles, denoted by the superscripts a and b , described by the unicycle kinematic model, whose state consists of their coordinates x, y in the world reference frame $\langle W \rangle$, and of their heading θ with respect to a reference axis. Their dynamics is described in discrete-time as in [15]

$$x_{k+1} = x_k + A_k C_k, \quad y_{k+1} = y_k + A_k S_k, \quad \theta_{k+1} = \theta_k + \omega_k T_s, \quad (1a)$$

with $A_k = \frac{2v_k}{\omega_k} \sin\left(\frac{T_s}{2}\omega_k\right)$ (where $\lim_{\omega_k \rightarrow 0} A_k = v_k T_s$), $C_k = \cos\left(\theta_k + \frac{T_s}{2}\omega_k\right)$ and $S_k = \sin\left(\theta_k + \frac{T_s}{2}\omega_k\right)$. The control inputs v_k and ω_k represent the forward and angular velocity respectively, while the subscript k denotes the k -th time instant kT_s , while T_s is the sampling period. Each vehicle is equipped with a range sensor with sensing range R , measuring its distance from its reference fixed-frame landmark $M_i = [X_i, Y_i]^\top$, $i = 1, 2$. Without loss of generality, we consider $M_1 = [0; 0]^\top$, and $M_2 = [D; 0]^\top$, with $D > 0$. Moreover, the vehicles can measure their relative distance whenever they come sufficiently close (within R) to each other. Therefore, the measurement model for the robots is

$$z_k^a = [\rho_{k,1}^2; \rho_k^2]^\top, \quad z_k^b = [\rho_{k,2}^2; \rho_k^2]^\top, \quad (1b)$$

with $\rho_k^{a2} = (x_k^a - X_1)^2 + (y_k^a - Y_1)^2$ if $\rho_k^a \leq R$, $\rho_k^{b2} = (x_k^b - X_2)^2 + (y_k^b - Y_2)^2$ if $\rho_k^b \leq R$, and with $\rho_k^2 = (x_k^a - x_k^b)^2 + (y_k^a - y_k^b)^2$ if $\rho_k \leq R$. For the sake of clarity, we introduce here a new notation to denote the reference frame that will be used in the forthcoming.

Notation: We denote the position of the vehicle a in the world reference frame $\langle W \rangle$ as $q_k^a = [x_k^a, y_k^a]^\top$ and its position sequence $Q^a = \{q_k^a\}$. Furthermore, we define by $\langle a(M_1) \rangle$ the reference frame centred in M_1 and with the x -axis aligned with one point of the trajectory followed by vehicle a that will be specified from time to time; the state of the vehicle a in $\langle a(M_1) \rangle$ will be denoted by p_k^a . The same definitions apply to vehicle b .

Remark 1: The knowledge of two positions $q_{k_1}^a$ and $q_{k_2}^a$, $k_1 < k_2$, and the knowledge of v_k and ω_k , $\forall k \in [k_1, k_2]$ together with the discrete dynamics (1) determine uniquely θ_k^a , $\forall k \in [k_1, k_2]$. Hence, the localisation problem can be recast into the reconstruction of two positions $q_{k_1}^a$ and $q_{k_2}^a$.

A. Theoretical background

We deal with the localisation of the vehicles in the world reference frame $\langle W \rangle$, by relying on the control inputs v_k, ω_k and on the measurement outputs z_k^a, z_k^b over a given time interval $[k_0, k_f]$. This task is associated with the concept of *u-indistinguishability*, introduced in the following definition.

Definition 1: Given a nonlinear discrete-time system $s_{k+1} = f(s_k, u_k)$, $z_k = h(s_k)$, a time interval $K = [k_0, k_f]$, and an admissible control input history u_k^* , $k \in K$, two states s_0 and \bar{s}_0 are said to be **u*-indistinguishable** if the output histories z_k and \bar{z}_k , $k \in K$ of the trajectories satisfying the initial conditions s_0 and \bar{s}_0 respectively, are identical.

To compact the notation, in the rest of the paper, we will refer to *indistinguishable trajectories* as trajectories having *u-indistinguishable* initial conditions.

The indistinguishability properties of the trajectories followed by a vehicle depend on the number of measurements that are collected, on their distribution among different fixed-frame landmarks, and on the manoeuvres executed by the vehicle itself. We recall here the analysis of indistinguishability of some trajectories followed by a vehicle with respect to an anchor, which will prove useful in the following analyses.

1) *Single anchor:* In our previous work [5], we have analysed the situation with a vehicle sensed by a single anchor, whose results are summarised in the following proposition:

Proposition 1: Given the vehicle a , its position sequence $Q^a = \{q_k^a\}$, $k = 0, \dots, N-1$, and the set of measurements ρ_k^a collected from anchor M_1 , a position sequence \bar{Q}^a is *u-indistinguishable* from Q^a if: (1) For any N , Q^a is a rotation of \bar{Q}^a about the anchor; (2) For $N = 2$ (or for $N > 2$ collinear measurement points), \bar{Q}^a is symmetric to Q^a with respect to an axis passing through the anchor.

By the analysis in [5], Proposition 1 collects the *sufficient and necessary* conditions for the case $N \geq 2$. In light of it, any measurement beyond the third, provided that the measurement points are noncollinear, adds no further information to the state of the vehicle. Indeed, the vehicle is aware of its distance from the anchor and of its orientation with respect to the line joining the anchor with the vehicle itself. Therefore, we consider this to be the condition where the vehicle has extracted the *maximum amount of information* from one anchor. On the other hand, when only 2 measurements are collected, the vehicle can compute a distance-orientation pair for each one of the two axial symmetric trajectories. This result will prove useful in the analysis with more anchors, presented hereafter.

2) *More anchors:* To compact the notation, we list the number of measurements collected from each anchor, divided by a “+” sign. With a 3 + 1 setting, i.e. 3 measurements from one anchor and 1 from another, the vehicle a is aware of its distance from the first anchor at any time. Thus, q_3^a , related to the second anchor, lies on an intersection between the circles centred in the two anchors, hence defining two indistinguishable sequences \bar{Q}^a and Q^a . With the same rationale, 2 measurements from the first anchor yield 2 potential distances from it, and thus a 2 + 1 setting yields a maximum number of 4 indistinguishable trajectories. When the indistinguishable trajectories are known, the vehicle can explicitly design a further manoeuvre to obtain a measurement ruling out the ambiguities. This procedure will be detailed out more in our specific case at the end of Section III.

B. Problem statement

Given the position of the two anchors M_1 and M_2 in $\langle W \rangle$, we aim at designing the manoeuvres of the two vehicles that solve the localisation problem. Furthermore, we will use the measurements collected along the trajectories and the sequence of manoeuvres executed by the vehicles to reconstruct their trajectories in $\langle W \rangle$.

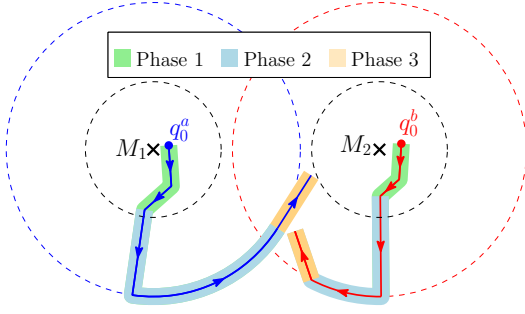


Fig. 1. Trajectory planning algorithm: the paths of the two vehicles are represented in blue and red respectively, while the three phases are highlighted with different colours. The black dashed lines represent the sensing range of the anchors, while coloured dashed lines represent the “orbiting” distance of the two vehicles, which will be defined in phase 2.

III. TRAJECTORY PLANNING ALGORITHM

The two vehicles a and b start from unknown initial positions q_0^a and q_0^b in the range of the respective anchor. Then, each vehicle implements its perception-aware trajectory planning algorithm to meet the other agent and share the collected information in order to simultaneously localise the agents. The planning algorithm comprises three main phases: (1) collecting the largest amount of information by the reference anchor, (2) meeting the other vehicle by “orbiting” about the anchors, (3) designing the last manoeuvres to avoid indistinguishability. The three phases are presented in Figure 1, and are described separately in the next sections.

A. Phase 1: Fixed-frame marker

In this phase, highlighted in green in Figure 1, the vehicles are far away from each other and cannot communicate or exchange information, thus they have to plan their trajectory separately. Without loss of generality, we will analyse vehicle a , dropping the superscript a for readability. At the initial time, the vehicle collects its distance ρ_0 from the anchor and has to determine v_0 and ω_0 to the second measurement point. To cope with a potential measurement noise, making two near points be sensed as a unique point, we plan the first manoeuvre to maximise the distance between q_0 and q_1 , by maximising A_0 in (1), i.e., $v_0 = v_{\max}$ and $\omega_0 = 0$. Since the vehicle is not aware of its position in $\langle W \rangle$, it may or may not collect ρ_1 at $k = 1$. The two cases are treated separately.

1) ρ_1 is collected after the first manoeuvre: If the vehicle remains in the sensing range of the anchor and collects the measurement ρ_1 , it can now build two position sequences, \mathcal{Q} and $\bar{\mathcal{Q}}$, compliant with the measurements and with the manoeuvres in its local reference frame $\langle a(M_1) \rangle$: $p_0 = [\rho_0, 0]^\top$, and $p_1 = [\rho_0 + A_0 \cos \alpha, \pm A_0 \sin \alpha]^\top$, with

$$\alpha = \arccos\left(\frac{\rho_1^2 - \rho_0^2 - A_0^2}{2\rho_0 A_0}\right), \quad (2)$$

yielding $\|p_0 - p_1\| = A_0$, and $\|p_1 - M_1\| = \rho_1$. From p_1 , the vehicle has to plan the next manoeuvre (v_1, ω_1) . By the definition of p_1 and by applying the controls, we can compute the distance from the anchor the robot will reach in p_2 , i.e.

$$d^2 = \Delta^2 + 2\rho_0 A_1 \cos(\pm\alpha + \delta_1), \quad (3)$$

where $\delta_1 = \omega_1 T_s / 2$ and $\Delta^2 = \rho_0^2 + A_0^2 + A_1^2 + 2A_0 A_1 \cos \delta_1 + 2\rho_0 A_0 \cos \alpha$, which yields two solutions, say d_+ and d_- . By Proposition 1, any pair (v_1, ω_1) , such that $v_1 \neq 0$, $\omega_1 \neq j\pi$, $j \in \mathbb{Z}$, is suitable to get the maximum amount of information. We design the pair (v_1, ω_1) maximising the difference

$$|d_+^2 - d_-^2| = 8\rho_0 \sin \alpha \frac{v_1}{\omega_1} \sin^2\left(\frac{T_s}{2}\omega_1\right).$$

This way, we maximise the intensity of a potential measurement noise that is necessary to “confuse” the two predicted distances with each other, thus increasing the robustness of this process to measurement noise. More precisely, we define

$$\max_{v_1, \omega_1} \frac{v_1}{\omega_1} \sin^2\left(\frac{T_s}{2}\omega_1\right), \quad \text{s.t. } |v_1| \leq v_{\max}, |\omega_1| \leq \omega_{\max}, \quad (4)$$

thus the optimal value of ω_1 can be found by computing the partial derivative of the cost function with respect to ω_1 and setting it to 0. This procedure yields $\cos(T_s \omega_1) + T_s \omega_1 \sin(T_s \omega_1) - 1 = 0$, whose solution cannot be found in closed form, but numerically yields $\omega_1 = 2.3311/T_s$. Since the optimisation problem in (4) is constrained, the optimal value for ω_1 is $\min\{2.3311/T_s, \omega_{\max}\}$. Although the forward velocity solving (4) is $v_1 = v_{\max}$, we have no guarantee that at least one of the two measurement points will fall in the sensing range of the anchor. However, by using (3), we can enforce that $\min\{d_+, d_-\}^2 \leq R^2$ by choosing v_1 as in (5). Hence, if the vehicle falls outside the sensing range, i.e., no measurement is collected, a *virtual measurement* $\rho_2 = \max\{d_-, d_+\}$ is collected. Therefore, by Proposition 1, with three non-collinear measurement points, the vehicle collects the largest amount of information from its reference anchor.

2) ρ_1 is not collected after the first manoeuvre: To collect the second measurement, the vehicle turns on the spot by $\pi/2$, i.e., $v_1 = 0$ and $\omega_1 = \frac{\pi}{2T_s}$, and starts moving on a circle with centre q_0 and radius A_0 , i.e., $v_k/\omega_k = A_0$, with $k = 2, \dots, k_\rho - 1$, where k_ρ is the time instant when the measurement is collected. Since q_0 is within the sensing range of the anchor and $A_0 < R$, an arc of the circular trajectory of the vehicle, with amplitude $2\pi - 2\eta$, will be inside the sensing range, leading the vehicle to collect the measurement ρ_1 , as in Figure 2(a), where $\eta = \arccos\left(\frac{R^2 - \rho_0^2 - A_0^2}{2A_0 \rho_0}\right)$. However, since measurements occur only at sampling times kT_s , the vehicle travels an arc of maximum amplitude $2\pi - 2\eta$ during T_s , hence upper-bounding its velocity to $\omega_k = \min\{\omega_{\max}, \frac{2\pi - 2\eta}{T_s}, \frac{v_{\max}}{A_0}\}$ and leading to the forward velocity $v_k = \omega_k A_0$. After N_l manoeuvres, the vehicle enters the sensing range of the anchor, collects ρ_1 , and computes α by using (2): this way, the vehicle can find two trajectories \mathcal{Q} and $\bar{\mathcal{Q}}$ (associated with $\pm\alpha$ as in the previous case), that are compliant with the measurements and the manoeuvres, hence indistinguishable. In the reference frame $\langle a(M_1) \rangle$, the vehicle can compute the coordinates, and consequently the distance d_l , of each point p_l in \mathcal{Q} and $\bar{\mathcal{Q}}$

$$d_l^2 = \rho_0^2 + A_0^2 + 2\rho_0 A_0 \cos(\pm\alpha - l\omega_k), \quad l = 1, \dots, N_l.$$

$$v_1 = \frac{\omega_1}{2 \sin\left(\frac{T_s}{2}\omega_1\right)} \left[\sqrt{R^2 - \left(\rho_0 \sin\left(\alpha + \frac{T_s}{2}\omega_1\right) + A_0 \sin\left(\frac{T_s}{2}\omega_1\right)\right)^2} - \rho_0 \cos\left(\alpha + \frac{T_s}{2}\omega_1\right) - A_0 \cos\left(\frac{T_s}{2}\omega_1\right) \right] \quad (5)$$

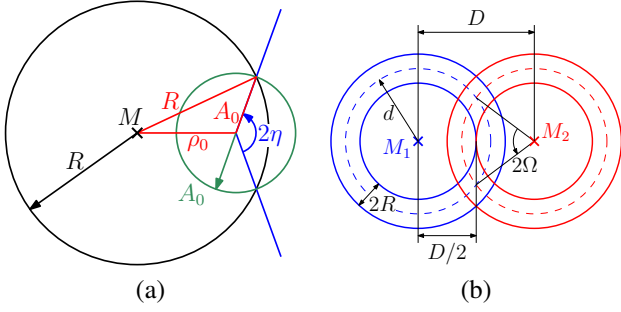


Fig. 2. (a) Phase 1, ρ_1 not collected after the first manoeuvre: Circular path followed by the vehicle after the first (straight) motion. (b) Phase 2: orbiting paths with the definitions of the angle Ω .

If one of these distances $d_l \leq R$, the corresponding trajectory is disregarded, thus collecting the largest amount of information from one anchor with only two measurements (see Figure 3(b)). Should this situation not happen, i.e., $d_l > R, \forall l = 1, \dots, N_l$, the vehicle can follow the same procedure as before to collect the third measurement ρ_2 , with the proper modifications accounting for its orientation.

B. Phase 2: Meeting the other vehicle

By Proposition 1, after the first phase, the two vehicles can now estimate their position p_k and determine their orientation μ with respect to the line joining the anchor and the vehicle itself in their reference frame $\langle a(M_1) \rangle$ and $\langle b(M_2) \rangle$, with

$$\mu = \begin{cases} \omega_2 T_s + \alpha - \arctan 2(y, x), & \text{with 3 measurements} \\ \frac{\pi}{2} + \alpha - \arctan 2(y, x), & \text{with 2 measurements} \end{cases},$$

where the x and y coordinates are known in the local $\langle a(M_1) \rangle$ and $\langle b(M_2) \rangle$ reference frames, and depend on the procedure followed in the first phase. Moreover, the distance from the anchor is known from the last measurement. To reach any prescribed distance from its anchor, the vehicle can turn by $-\mu$ on the spot (i.e. $v = 0, \omega = -\mu/T_s$), to align to the diameter of the circle centred in the reference anchor, and travel on a straight path, i.e. $\omega = 0$. The vehicles are aware of their radial coordinates with respect to their reference anchor and of the distance D between the two anchors themselves, and have to plan their trajectories in order to reduce their relative distance below the sensing range R . To this aim, the two vehicles travel on a circular trajectory, centred in their reference anchor, with prescribed radius d , as reported in Figure 1, highlighted in light blue. To determine the optimal radius d , we consider the situation represented in Figure 2(b) where the vehicles and the anchors are aligned on the x -axis of $\langle W \rangle$, with horizontal coordinates $X_1 = 0, x_a = d, x_b = D - d, X_2 = D$, where we want the two vehicles to have distance R , and $x_a > x_b$, and thus $d = \frac{D+R}{2}$. We then define $\Omega = \arccos\left(\frac{D}{D+R}\right)$ as half of the angle described by the two segments connecting one of the anchors with the two intersections of the trajectories, giving an estimate of the arc where the measurement between

the two vehicles can occur. To meet, the vehicles rotate in opposite directions, choosing their velocities such that while a travels over a circle, b travels an arc with amplitude 2Ω ,

$$\begin{aligned} \omega_a &= \min \left\{ \omega_{\max}, \frac{2v_{\max}}{D+R} \right\}, & v_a &= \omega_a \frac{D+R}{2}, \\ \omega_b &= -\frac{\Omega}{\pi} \omega_a, & v_b &= -\omega_b \frac{D+R}{2}. \end{aligned} \quad (6)$$

With this choice of the control inputs, we can estimate an upper bound T_{\max} to the time needed by the two vehicles to meet, based on the time needed by b to travel over the entire circle, travelling twice on the 2Ω arc, yielding

$$T_{\max} = \frac{2\pi + 2\Omega}{|\omega_b|} = 2\pi \left(\frac{\pi}{\Omega} + 1 \right) \max \left\{ \frac{1}{\omega_{\max}}, \frac{D+R}{2v_{\max}} \right\}.$$

C. Phase 3: Designing the last manoeuvres

As soon as the two vehicles meet and collect the first mutual measurement $\rho_{1,m}$, they are aware of their sequence \mathcal{Q} in their local reference frame, of their distance, and of the distance D between the two anchors. Let p_1^a and p_1^b be the positions of the vehicles when the $\rho_{1,m}$ is collected. We define the local reference frame $\langle a(M_1) \rangle$ such that $M_1 = [0, 0]^T$ and $p_1^a = \left[\frac{D+R}{2}, 0\right]^T$. With the same procedure, in $\langle b(M_2) \rangle$, $M_2 = [0, 0]^T$ and $p_1^b = \left[\frac{D+R}{2}, 0\right]^T$, while the heading of the two vehicles with respect to their x -axis is $\pm\pi/2$ since they are travelling on the circle centred in their reference anchor. In $\langle b(M_2) \rangle$, we can regard M_2 and p_1^b as fixed-frame anchors, and thus the two distances D and $\rho_{1,m}$ generate a $1 + 1$ setting (see Section II) for the vehicle a .

a) *Second mutual measurement*: With the same rationale, we can treat the next position p_2^b of vehicle b as an additional anchor in $\langle b(M_2) \rangle$. Therefore, by collecting an additional measurement, we add no further information if the two vehicles do not move, while we have a $2 + 1$ if one of the two stays still, and a $1 + 1 + 1$ if both vehicles move. By the analysis in [5], a $2 + 1$ setting should be preferred, since it yields a number $N_{IT}^{[2+1]} \leq 4$ of indistinguishable trajectories that can be computed by checking a condition that will be detailed out later, while a setting $1 + 1 + 1$ yields $N_{IT}^{[1+1+1]} \leq 8$ indistinguishable trajectories, where $N_{IT}^{[1+1+1]}$ cannot be computed. Therefore, vehicle b stops as soon as it collects the first measurement (i.e. $p_2^b = p_1^b$), while vehicle a follows the same procedure as in the first phase to collect a second mutual measurement, i.e. moving straight and possibly travelling on a circle centred in its previous position. With these manoeuvres, we can update the reference frame $\langle a(M_1) \rangle$, by adding the known position $p_2^a = p_1^a + [\delta x, \delta y]^T$, and define γ as the angle described by the two branches of \mathcal{Q}_a intersecting in p_1^a as $\gamma = \pi - \arctan 2(\delta y, \delta x)$. To compute the number of indistinguishable trajectories arising in this $2 + 1$ setting, we build a reference frame where p_1^b lies on the origin, while p_1^a lies on the x -axis, i.e. $\langle a(p_1^b) \rangle$, which will allow us to compute the distance $\|M_1 - p_1^b\|$. In this frame, $p_1^a = [\rho_{1,m}, 0]^T$, $p_2^a = p_1^a + A_1[\cos \alpha, \pm \sin \alpha]^T$ and

$$M_1 = p_1^a + \frac{D+R}{2} [\cos(\pm\alpha + \gamma); \sin(\pm\alpha + \gamma)]^T,$$

and thus, we conclude that

$$\|M_1 - p_1^b\|^2 = \left(\frac{D+R}{2}\right)^2 + \rho_{1,m}^2 + \rho_{1,m}(D+R)\cos(\pm\alpha + \gamma).$$

Therefore, in $\langle b(M_2) \rangle$, the landmark M_1 lies at the intersection between one of the two circles centred in p_1^b with radius $\|M_1 - p_1^b\|$ and the circle centred in M_2 with radius D . We can compute the number of intersections between the circles. In particular, each circle centred in M_1 has 2 intersections if $\|M_1 - p_1^b\| \in (|D - R|/2, (3D + R)/2)$, hence fixing the maximum number of indistinguishable trajectories to 4. If the vehicle collects the second mutual measurement after travelling over a circular arc, it may be able to discard either α or $-\alpha$, hence yielding 2 indistinguishable trajectories. We remark that each of these *indistinguishable* sequences \mathcal{Q}_a can be roto-translated from $\langle b(M_2) \rangle$ to $\langle W \rangle$, since the coordinates of all the positions, including M_1 , are known.

b) *Third mutual measurement*: The indistinguishable sequences \mathcal{Q}^a in $\langle b(M_2) \rangle$ can be built by using the solutions $\phi, \Delta x, \Delta y$ of the following set of equations

$$\begin{aligned} \|M_2 - (\mathcal{R}_\phi M_1 + T)\|^2 &= D^2 \\ \|p_1^b - (\mathcal{R}_\phi p_k^a + T)\|^2 &= \rho_{k,m}^2, \quad k = 1, 2, \end{aligned} \quad (7)$$

where $\mathcal{R}_\phi = \begin{bmatrix} \cos \phi & -\sin \phi \\ \sin \phi & \cos \phi \end{bmatrix}$ is a rotation matrix, $T = [\Delta x, \Delta y]^\top$ is a translation vector, M_1, p_1^a and p_2^a are expressed in $\langle a(M_1) \rangle$, while M_2, p_1^b and p_2^b in $\langle b(M_2) \rangle$. To this end, it is convenient to subtract the first equation from the others, yielding two linear equations in Δx and Δy , substitute the result into the first equation, thus having a nonlinear equation in ϕ with a known number of solutions. Once the $N \leq 4$ solutions to (7) are found, vehicle b is aware of the possible positions $p_{2,i}^a, i = 1, \dots, N$ in $\langle b(M_2) \rangle$. For simplicity's sake, a stops as soon as it collects $\rho_{2,m}$. Vehicle b plans (v_2, ω_2) and moves to the next point p_2^b , whose distance d from vehicle a is one of the N possible $d_i = \|p_{2,i}^a - p_2^b\|$. As in the previous analysis, to cope with measurement noise, b plans its manoeuvre such that the predicted measurements d_i are as far as possible from each other, thus defining the optimisation problem

$$\max_{v_2, \omega_2} J, \quad \text{s. t.} \quad |v_2| \leq v_{\max}, |\omega_2| \leq \omega_{\max}, \quad (8)$$

where $J = \min_{(i,j)} |d_i - d_j|$ is linear in v_2 , indeed with $v_2 = 0$ the vehicles collect the same measurement $\rho_{2,m}$, and thus we select $v_2 = v_{\max}$. For each pair of possible positions of vehicle a in $\langle b(M_2) \rangle$, we can compute the difference of the distances as a function of ω_2 . However, the cost J is defined piecewise, due to the $\min(\cdot)$ operator, and thus a closed-form solution cannot be found. Therefore, we deal with this problem by enumeration: we select a sufficiently high number of values for ω_2 and, for each of them, we determine and choose the smallest difference of distances, which gives us the value of ω_2 corresponding to the maximum value of the cost function J obtained through this procedure. Once v_2 and ω_2 are selected, vehicle b moves and collects the last mutual measurement, which rules out the ambiguity between the N possible positions p_2^a . The global localisation problem is thus solved using the planned trajectories.

IV. SIMULATION EXAMPLES

We present here two different examples, with the same parameters $R = 3$ m, $D = 10$ m, $T_s = 1$ s, $v_{\max} = 1$ m/s and $\omega_{\max} = \pi$ rad/s, with different initial conditions. Different initial states will lead the vehicles to take different decisions, thus covering all the described cases. We remark that the representation of the trajectories will consist in a line connecting the successive positions of the vehicles, while the path followed by the vehicles (see discretisation in (1a)), consists of straight lines and arcs of circles.

1) *First simulation*: In the first simulation example, in Figure 3, we choose the initial conditions as $s_0^a = [2.4, -1.2, 4.8]^\top$, $s_0^b = [11.3, -0.4, 3.6]^\top$. Figure 3(a) shows the position sequences \mathcal{Q}_a in blue and \mathcal{Q}_b in red, during the whole simulation. Phase 1 of vehicle a is described in Figure 3(b), where the vehicle moves straight falling outside the sensing range of M_1 , represented by the solid black line, travels on a circle and eventually collects the second measurement. These two measurements are sufficient to collect the maximum amount of information from the anchor, since the dotted trajectory, associated with $-\alpha$, has points inside the sensing range that should have been sensed by the anchor, thus allowing vehicle a to avoid the potential ambiguity $\pm\alpha$. The same outcome is obtained by b by collecting three measurements from M_2 . During phase 2, the two vehicles reach their orbiting distance, dashed red and blue lines in Figure 3(a), until they meet. A screenshot of the first mutual measurement is reported in Figure 3(d1), where b stops, while a proceeds straight, i.e. on the tangent of its orbiting circle, as depicted in Figure 3(d2). After the second mutual measurement, vehicle a stops, while b finds the 4 potential trajectories followed by a in $\langle b(M_2) \rangle$, getting to the setting in Figure 3(c), thus finding the optimal value for ω_2 , maximising the smallest difference of the distances, generating the motion in Figure 3(d3). Despite the natural intuition, vehicle b does not move on the bisector between two axes in Figure 3(c), but it seeks for a trade-off between this behaviour and the maximum possible displacement.

2) *Second simulation*: For the second simulation example, presented in Figure 4, we choose the initial conditions $s_0^a = [-1.5, -1.7, 2.6]^\top$, $s_0^b = [10, -0.1, 6]^\top$. In phase 1 the two vehicles collect 3 measurements each from their reference anchors, then reach the prescribed orbiting distance (phase 2). The noteworthy difference with the previous example occurs in phase 3. Indeed, by following a straight path, vehicle a falls outside the sensing range of b , travels over a circle, and eventually falls inside the sensing range of b , ruling out the ambiguity $\pm\alpha$ in (3), thus decreasing to 2 the number of indistinguishable trajectories. Vehicle b plans its last manoeuvre in the same way as before, maximising the only difference of the two distances, as in Figure 4(b).

V. CONCLUSIONS

We have proposed a control algorithm for a pair of vehicles, unaware of their initial state in the space, allowing them to localise themselves in the environment. Each of them collects information from its reference anchor, navigates in

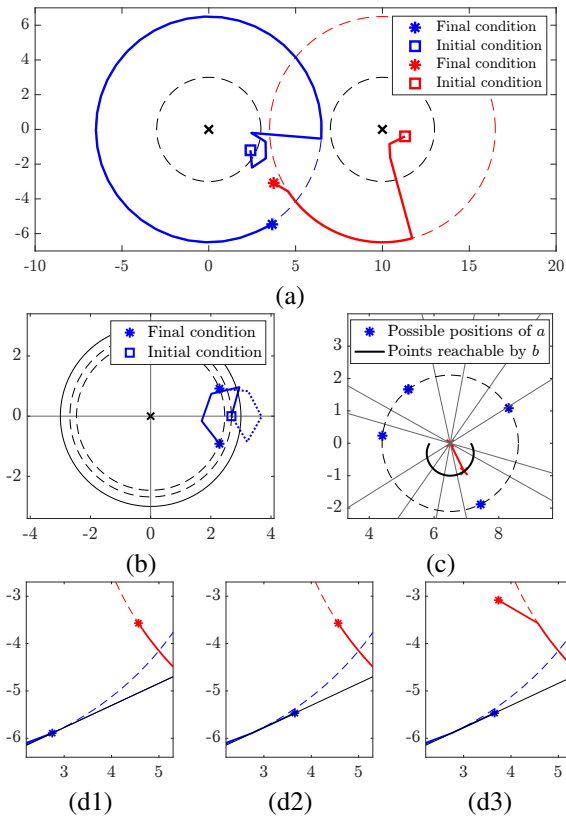


Fig. 3. First simulation example. (a) Path followed by vehicle a in blue, and by b in red. The black crosses the position of the two landmarks M_1 , M_2 , with sensing range R (black dashed line), whereas the dashed lines represent the orbiting distances. (b) Phase 1: $\langle a(M_1) \rangle$, two trajectories $\pm\alpha$ of vehicle a , where the solid line represents the sensing range R , the dashed lines represent the measurements ρ_0 (outer) and ρ_1 (inner). The dotted trajectory is discarded, since some of its points are inside the sensing range. (c) Phase 3: $\langle b(M_2) \rangle$ after the second mutual measurement. The black solid line represents the points reachable by b with $v_2 = v_{\max}$, the red line and the red crosses denote the best choice for ω_2 , the blue dots are the four potential positions of the vehicle a , with distance ρ_2 denoted by the black dashed line, while the thin black lines represent the axes of the segments with a pair of blue dots as endpoints. (d) Phase 3, zoom from (a): the vehicles collect their first mutual measurement (d1), a moves on the tangent (black solid line) of the dashed circle (d2), and eventually b moves according to the control inputs described in (c), i.e. turning slightly left.

the environment with a reduced knowledge of its state until the two vehicles meet. As soon as they meet, they plan their last two manoeuvres that are needed to collect the necessary information on their state. In this work, the two vehicles rely on known and perfect actuation and communication: we plan to analyse the same scenario as in this case, considering also process noise or a malicious agent that broadcasts wrong information on the executed manoeuvres.

REFERENCES

- [1] P. Chen, Y. B. Xu, L. Chen, and Z. A. Deng, "Survey of WLAN fingerprinting positioning system," *Applied Mechanics and Materials*, vol. 380, pp. 2499–2505, Aug. 2013.
- [2] P. Nazemzadeh, F. Moro, D. Fontanelli, D. Macii, and L. Palopoli, "Indoor Positioning of a Robotic Walking Assistant for Large Public Environments," *IEEE Trans. on Instrumentation and Measurement*, vol. 64, no. 11, pp. 2965–2976, Nov 2015.
- [3] K. Cheok, M. Radovnikovich, P. Vempaty, G. Hudas, J. Overholt, and P. Fleck, "UWB tracking of mobile robots," in *Proc. IEEE*

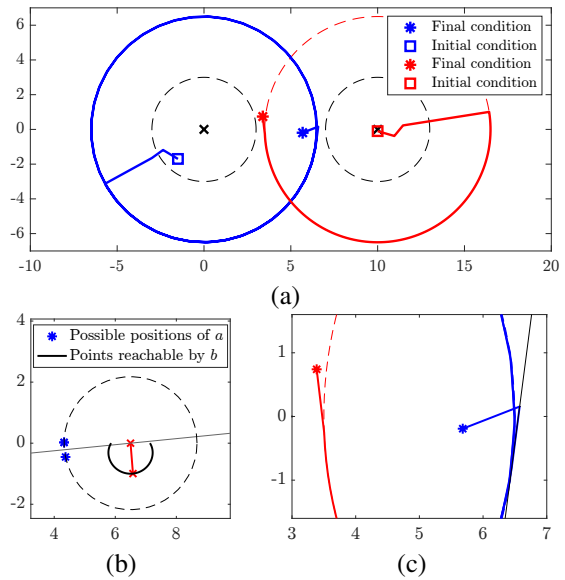


Fig. 4. Second simulation example. (a) Paths followed by the two vehicles. (b) Phase 3: Situation seen by vehicle b while planning its last manoeuvre, with the same conventions as in Figure 3. The possible positions of vehicle a are reduced to 2, since it has followed a curved trajectory outside the sensing range of b (similar to the one in Figure 3(a)), thus ruling out the ambiguity between the two trajectories. (c) Phase 3: zoom on the last points reached by the two vehicles.

- [4] F. Riz, L. Palopoli, and D. Fontanelli, "On local/global constructibility for mobile robots using bounded range measurements," *IEEE Control Systems Letters*, 2022.
- [5] —, "Analysis of indistinguishable trajectories of a nonholonomic vehicle subject to range measurements," 2022. [Online]. Available: <https://arxiv.org/abs/2209.00567>
- [6] S. Cedervall and X. Hu, "Nonlinear observers for unicycle robots with range sensors," *IEEE transactions on automatic control*, vol. 52, no. 7, pp. 1325–1329, 2007.
- [7] P. Salaris, M. Cognetti, R. Spica, and P. R. Giordano, "Online optimal perception-aware trajectory generation," *IEEE Transactions on Robotics*, vol. 35, no. 6, pp. 1307–1322, 2019.
- [8] O. Napolitano, D. Fontanelli, L. Pallottino, and P. Salaris, "Information-aware Lyapunov-based MPC in a feedback-feedforward control strategy for autonomous robots," *IEEE Robotics and Automation Letters*, vol. 7, no. 2, pp. 4765–4772, April 2022.
- [9] N. De Carli, P. Salaris, and P. R. Giordano, "Online decentralized perception-aware path planning for multi-robot systems," in *2021 International Symposium on Multi-Robot and Multi-Agent Systems (MRS)*. IEEE, 2021, pp. 128–136.
- [10] D. Coleman, S. D. Bopardikar, and X. Tan, "Observability-aware target tracking with range only measurement," in *2021 American Control Conference (ACC)*. IEEE, 2021, pp. 4217–4224.
- [11] N. T. Hung and A. M. Pascoal, "Range-based navigation and target localization: Observability analysis and guidelines for motion planning," *IFAC-PapersOnLine*, vol. 53, no. 2, pp. 14 620–14 627, 2020.
- [12] F. Mandić, N. Mišković, N. Palomeras, M. Carreras, and G. Vallicrosa, "Mobile beacon control algorithm ensures observability in single range navigation," *IFAC-PapersOnLine*, vol. 49, no. 23, pp. 48–53, 2016.
- [13] R. Sharma, "Observability based control for cooperative localization," in *2014 International Conference on Unmanned Aircraft Systems (ICUAS)*. IEEE, 2014, pp. 134–139.
- [14] R. Boyinine, R. Sharma, and K. Brink, "Observability based path planning for multi-agent systems to aid relative pose estimation," in *2022 International Conference on Unmanned Aircraft Systems (ICUAS)*. IEEE, 2022, pp. 912–921.
- [15] L. Palopoli and D. Fontanelli, "Global observability analysis of a nonholonomic robot using range sensors," in *2020 European Control Conference (ECC)*. IEEE, 2020, pp. 1300–1305.